

## 2 **Supplementary Information for**

### 3 **Direct observation of crystallization and melting with colloids**

4 **Hyerim Hwang, David A. Weitz, and Frans Spaepen**

5 **Frans Spaepen.**

6 **E-mail: [spaepen@seas.harvard.edu](mailto:spaepen@seas.harvard.edu)**

#### 7 **This PDF file includes:**

- 8     Supplementary text
- 9     Figs. S1 to S6
- 10    Tables S1 to S2
- 11    Captions for Movies S1 to S2
- 12    References for SI reference citations

#### 13 **Other supplementary materials for this manuscript include the following:**

- 14     Movies S1 to S2

15 **Supporting Information Text**

16 **Phase behavior of repulsive charged colloids.** Long range repulsive interactions between particles are introduced by the  
17 addition of AOT surfactant molecules. The AOT molecules form inverse micelles above a critical concentration, which act as  
18 carriers. As a consequence, the particles are charged and the solvent conducts. Increasing the AOT concentration has two  
19 competing effects: The surface charge of the particles increases, thereby increasing the repulsive interaction between them.  
20 Simultaneously, the screening of the surface charge by charges in the solvent also increases, thereby reducing the range of their  
21 interaction. Increasing the concentration of AOT results in the sequential transformation of the fluid into a BCC, and FCC  
22 and then again fluid phase (reentrant melting). The phase diagrams are still inconsistent. Our phase stability is consistent  
23 with Ref.(1), but not with Ref.(2).

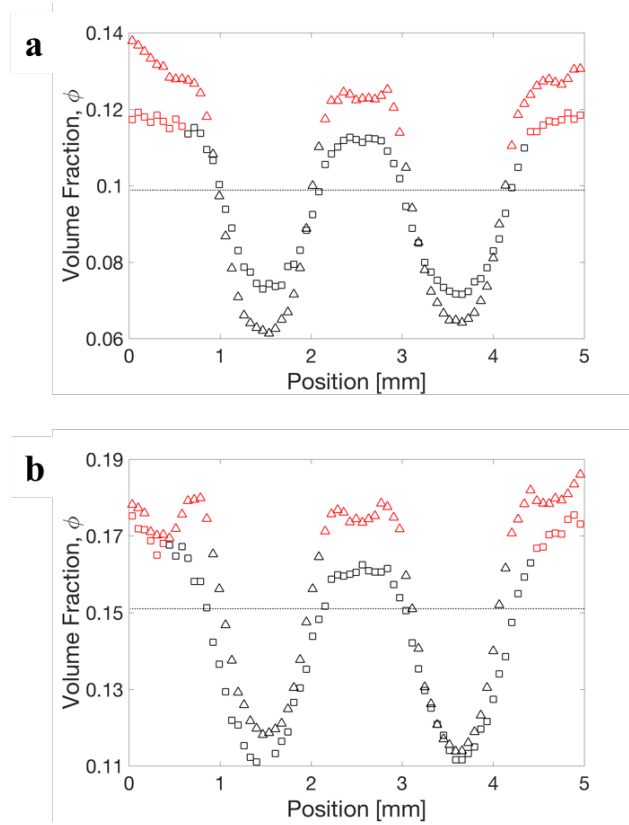


**Fig. S1. Volume fraction profile at dielectrophoretic equilibrium. a,** 15 mM AOT suspension forms BCC crystals. **b,** 5 mM AOT suspension forms FCC crystals. (red: crystalline, black: liquid, squares: 60 V, triangles: 80 V, dashed line: original packing fraction.)

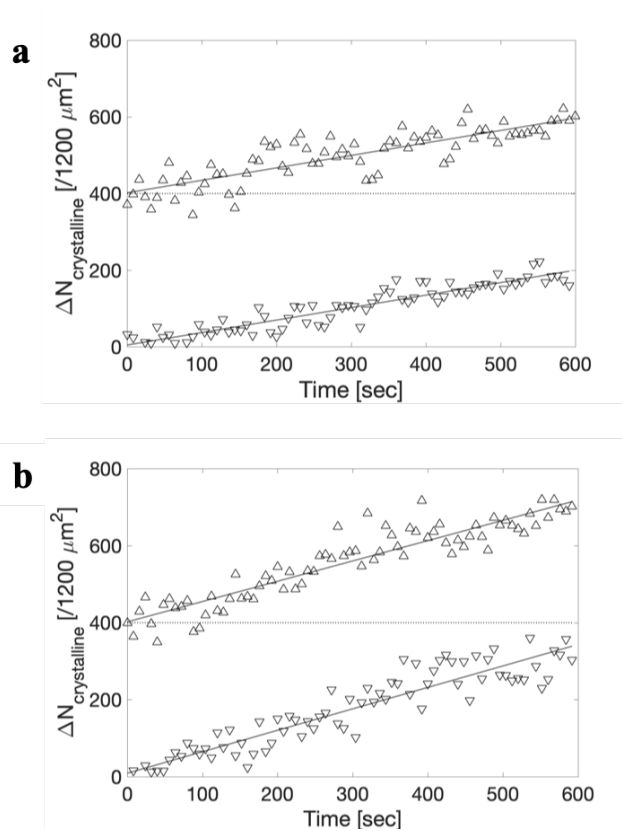


**Fig. S2. Crystal growth (change in the number of crystal particles) under two electrical conditions.** Down triangle ( $\nabla$ ) at 60 V and up triangle ( $\triangle$ ) at 80 V. **a**, BCC growth ( $v_{60V} = 0.331 \pm 0.020$  /sec,  $v_{80V} = 0.330 \pm 0.034$  /sec). **b**, FCC growth ( $v_{60V} = 0.584 \pm 0.044$  /sec,  $v_{80V} = 0.527 \pm 0.050$  /sec). Each point represents the increase for 8 seconds.

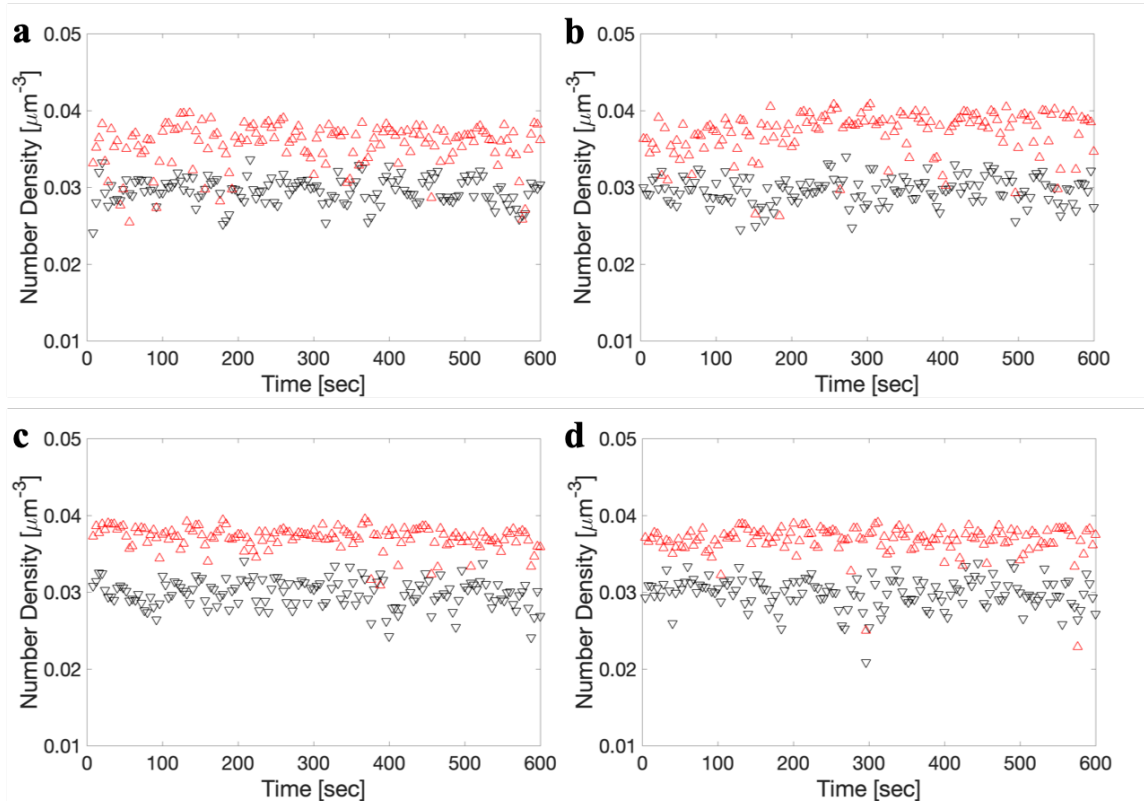


**Fig. S3.** Densities near the interface in the crystal and liquid during BCC melting and growing experiments at 60 V and 80 V. 1st row (a, b) and 2nd row (b, d) are the growing and melting, respectively. **a,c** 60 V. **b,d** 80 V. (red up triangle: crystal, black down triangle: liquid.)

The experiments were carried out at two voltages to ascertain that the electric field had no effect other than to control the densities. It was possible to create close to identical density gradients at both voltages, which show the same melting and solidification speeds, as well as jump rates.

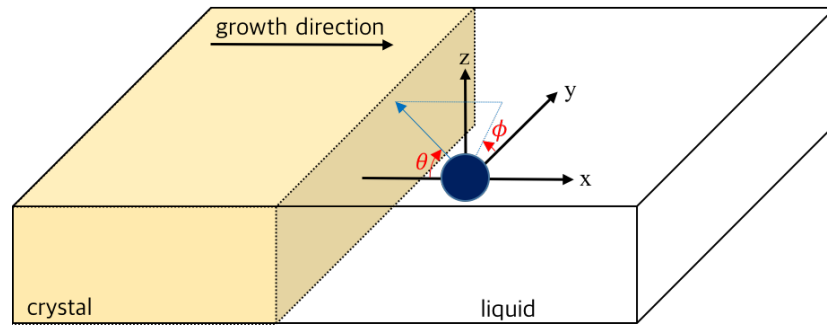
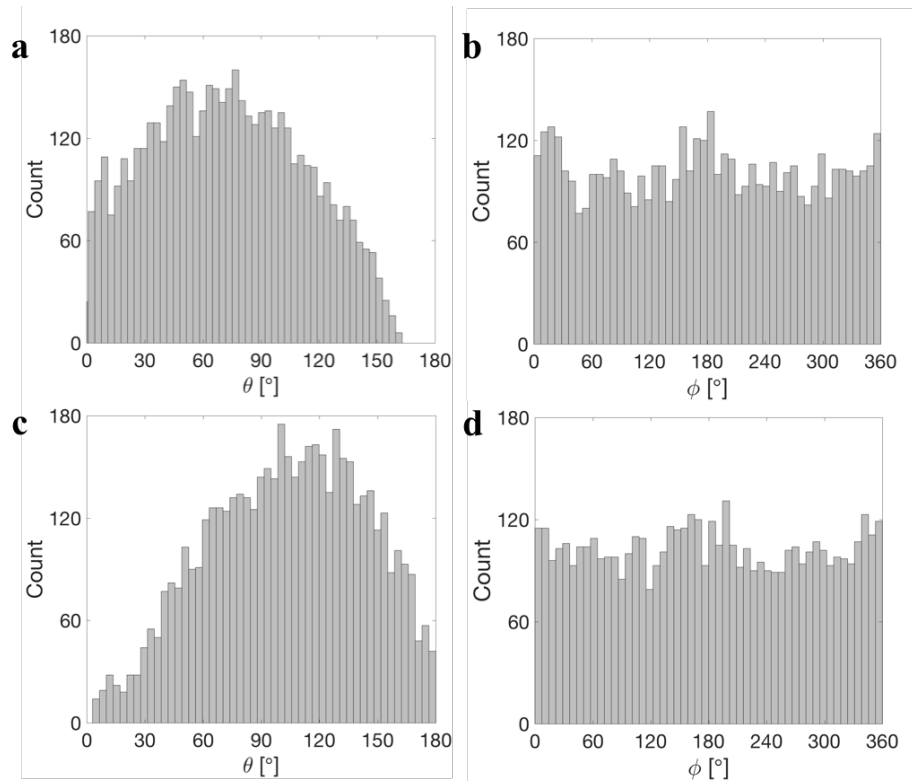
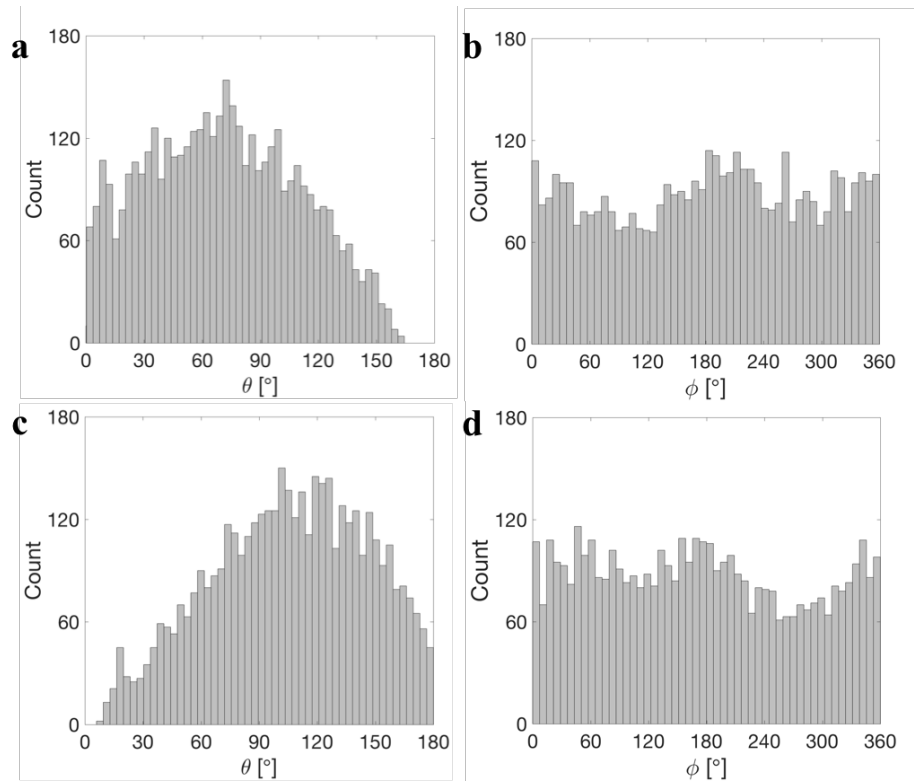


Fig. S4. 3D diagram of the azimuthal angle  $\phi$  ( $0 \leq \phi \leq 360$ ) and inclination angle  $\theta$  ( $0 \leq \theta \leq 180$ ) for an attachment or detachment jump (blue arrow). The results are shown in Figs. S5 and S6.



**Fig. S5. Angular distribution of the direction of the jumps at the BCC-liquid interface at equilibrium.** 1st column (a, c) and 2nd column (b, d) are the inclination angle,  $\theta$ , and azimuthal angle,  $\phi$ , respectively, with the x-axis along the growth direction. **a, b**, attachment. **c, d**, detachment.



**Fig. S6. Angular distribution of the direction of the jumps at the FCC-liquid interface at equilibrium.** 1st column (a, c) and 2nd column (b, d) are the inclination angle,  $\theta$ , and azimuthal angle,  $\phi$ , respectively, with the x-axis along the growth direction. **a, b**, attachment. **c, d**, detachment.



**Table S1. Average Voronoi volumes of particles in the crystal, interface, and liquid.**

Voronoi volume [ $\mu\text{m}^3$ ]		Equilibrium	Growth	Melting
BCC	Crystalline	$28.07 \pm 0.01$	$28.42 \pm 0.01$	$28.69 \pm 0.01$
	Interface	$28.17 \pm 0.03$	$28.47 \pm 0.02$	$28.77 \pm 0.03$
	Liquid	$28.30 \pm 0.02$	$28.74 \pm 0.01$	$28.89 \pm 0.02$
FCC	Crystalline	$19.38 \pm 0.01$	$18.35 \pm 0.01$	$19.48 \pm 0.01$
	Interface	$19.73 \pm 0.02$	$18.52 \pm 0.01$	$19.83 \pm 0.01$
	Liquid	$19.89 \pm 0.01$	$18.71 \pm 0.01$	$20.14 \pm 0.01$

**Table S2. Nearest neighbor distances (in  $\mu\text{m}$ ) determined from the average crystal Voronoi volumes ( $V_p$ ) (1st column) and from direct measurements of distances on the raw data (2nd column). BCC:  $d_{nn} = \frac{\sqrt{3}}{2}(2V_p)^{1/3}$ ; FCC:  $d_{nn} = \frac{\sqrt{2}}{2}(4V_p)^{1/3}$ . The values agree closely.**

	Nearest neighbor distances [ $\mu\text{m}$ ]	
BCC crystals	$3.30 \pm 0.08$	$3.32 \pm 0.55$
FCC crystals	$3.01 \pm 0.07$	$3.06 \pm 0.41$

24 **Movie S1. Growth of the BCC crystal of Fig. 2e.**

25 **Movie S2. Growth of the FCC crystal of Fig. 2f.**

26 For both movies, images were taken at 4 second intervals.

27 **References**

- 28 1. Sprakel J, Zaccone A, Spaepen F, Schall P, Weitz DA (2017) Direct observation of entropic stabilization of bcc crystals  
29 near melting. *Physical Review Letters* 118(8):088003.
- 30 2. Kanai T, et al. (2015) Crystallization and reentrant melting of charged colloids in nonpolar solvents. *Physical Review E*  
31 91(3):030301(R).